RSC Advances

PAPER

View Article Online
View Journal | View Issue

Cite this: *RSC Adv.*, 2026, **16**, 16963

Innovation in microbial bioactive materials: electrospun ectoine/ε-PL/PVA fiber dressing as a bioactive and hemocompatible material with potential for wound healing applications

Hamidreza Hagh Ranjbar and Afrouzossadat Hosseini Abari*

Bioactive fibers are innovative natural therapeutics, which are capable of mimicking the body's biological environment to accelerate healing, fight infections, and revolutionize regenerative medicine with extraordinary precision and effectiveness. In this study, we produced ectoine and epsilon-poly-L-lysine using *Halomonas elongata* and *Streptomyces albulus*, respectively, and utilized these compounds to fabricate ectoine/epsilon-poly-L-lysine/polyvinyl alcohol fibers *via* electrospinning for the development of a multifunctional wound dressing. The physicochemical properties of the biofibers were characterized using Field Emission Scanning Electron Microscopy (FE-SEM), differential scanning calorimetry (DSC), and Attenuated Total Reflectance-Fourier Transform Infrared Spectroscopy (ATR-FTIR). Additionally, their antibacterial, antibiofilm, antioxidant, and cytotoxic effects were evaluated. The potential of these biofibers as wound dressings was further assessed through hemocompatibility testing, *in vitro* scratch assay, and gene expression analysis during *in vitro* scratch-induced gap closure by qRT-PCR on L929 fibroblast cell cultures. The results of this study confirmed the fabrication of smooth, regular, and bead-free microfibers with a size of 0.8 ± 0.157 μm. These biofibers also exhibited significant biological activity without any toxicity or blood incompatibility. Finally, the induction of cell migration and the increased expression of matrix metalloproteinase-9 (MMP-9) and Transforming Growth Factor beta (TGF-β) demonstrate the potential of this biofiber as a bioactive wound dressing. The results of this study indicate the promising potential of ectoine/epsilon-poly-L-lysine/polyvinyl alcohol biofiber as bioactive, hemocompatible, and multifunctional wound dressings for advanced biomedical applications.

Received 9th December 2025
Accepted 3rd March 2026

DOI: 10.1039/d5ra09550f

rsc.li/rsc-advances

1. Introduction

Biocomposites are innovative materials that have gained significant interest in recent years due to their biocompatibility, biodegradability, and non-toxicity.[1] These composites, which are obtained from the synergy of biopolymers and reinforcing agents, have led to the development of new materials with unique properties.[2] There are various methods for preparing biocomposites, including laser printing, extrusion, grafting, phase separation, melt mixing, filament winding, solvent casting, and electrospinning.[3] Electrostatic fiber spinning (also known as electrospinning) is a sophisticated and versatile technique that applies high electric voltage to fabricate nano- or microscale materials.[4] Microfibers with high specific surface area, controllable permeability, and appropriate absorbency are potential candidates for use in various food, medical, textile, and pharmaceutical industries.[1,3] Moreover, integrating bioactive compounds into microfibers during synthesis can impart additional functionalities such as antimicrobial, anti-cancer, anti-inflammatory, and antioxidant properties.[5]

Bioactive compounds are natural products synthesized by a wide range of living organisms, including plants, fungi, and bacteria.[6] Bacteria convert various organic sources into intracellular and extracellular metabolites, which are considered potential candidates for use in different scientific and industrial fields due to their high production capacity and bioactive effects.[7] Ectoine 4,5,6-tetrahydro-2-methyl-4-pyrimidine-carboxylic acid (ECT) is a natural protective molecule found in some extremophilic microorganisms that protects against various harsh and extreme environmental conditions, such as salinity, heat, dryness, and ultraviolet radiation.[8] This low molecular weight cyclic amino acid derivative has gained prominence among many researchers and industrialists due to its anticancer, antioxidant, and especially anti-inflammatory effects.[9] The protective effect of ECT, which is achieved through water binding and complex formation, is driven by an entropy-based mechanism called "preferential elimination" or "preferential hydration", which affects the properties of the

Department of Cell and Molecular Biology & Microbiology, Faculty of Biological Science and Technology, University of Isfahan, Isfahan, Iran. E-mail: af.hosseini@sci.ui.ac.ir

"water shell" surrounding biomolecules.[10] It seems that exploiting this property and combining it with other bioactive compounds could lead to synergistic bioactive effects.

In addition to bacterial metabolites like ECT, bacterial polymers also serve as promising materials for biofiber synthesis. Epsilon-poly-L-lysine (ε-PL) is a homo biopolymer that consists of 25–35 lysine residues that are linked together by peptide bonds.[11] The ε-PL exhibits notable properties, including water solubility, biodegradability, safe for consumption, and non-toxicity to humans and the environment.[12] Within the last few years, ε-PL has been distinguished as an important biopolymer with potential applications in various industrial and medical fields, including food, medicine, environmental science, and electronics.[13] Numerous studies have shown its physicochemical characteristics as well as its antimicrobial, antioxidant, and anticancer properties, often demonstrating synergistic effects when combined with other compounds.[12,14,15] Among its well-recognized uses are enhancing food safety, dietary supplementation, fiber development, drug and gene delivery, and promoting skin regeneration.[16]

Considering the complementary physicochemical traits of ECT and ε-PL, such as their water-complexing behavior, targeted health-protective mechanisms, and significant biological activities, the combination of these two bioactive agents offers a compelling opportunity for advancing biofiber technology. Given the unique properties of these compounds, our goal was to create a new biodegradable and non-toxic bioactive compound with multiple applications. In this case, we synthesized a novel electrospun fiber, ECT/ε-PL/PVA, and conducted a comprehensive evaluation of its potential as an advanced wound dressing. Beyond a thorough characterization of its physicochemical and morphological properties, we rigorously assessed its multifaceted bioactivity, including potent antibacterial, antioxidant, and anticancer effects. Critically, its practical efficacy was confirmed through hemocompatibility tests, scratch assay, and quantitative real-time PCR (qRT-PCR) analysis of scratch-induced gap closure related genes.

2. Materials and methods

2.1. Ectoine production

The bacterial milking process was used to produce ECT from *Halomonas elongata* IBRC-M 10216 (ATCC 33173). First, the cells were grown in nutrient broth (Ibresco, Iran) containing 20% [W/V] NaCl (Neutron Chemical, Iran) at 30 °C and 150 rpm for 24 hours. Then, the culture was centrifuged at 800 RCF for 10 minutes (Hermle Z300-K; Germany), and the pellet was transferred to nutrient broth with 5% [W/V] NaCl. After 24 hours of incubation at 30 °C and 150 rpm, the produced ECT was separated and purified using the ethanol crystallization method described by Wei *et al.*[17]

2.2. Epsilon-poly-L-lysine production

The ε-PL was produced from *Streptomyces albulus* through a fermentation process in M3G medium (glucose 10 g L^{-1}, glycerol 15 g L^{-1}, $(NH_4)_2SO_4$ 10 g L^{-1}, yeast extract 5 g L^{-1}, Na_2HPO_4 1.6 g L^{-1}, K_2HPO_4 0.8 g L^{-1}, KH_2PO_4 1.4 g L^{-1}, $MgSO_4 \cdot 7H_2O$ 0.5 g L^{-1}, $ZnSO_4 \cdot 7H_2O$ 0.04 g L^{-1}, and $FeSO_4 \cdot 7H_2O$ 0.03 g L^{-1}). The culture was incubated at 30 °C, 150 rpm for 168 hours. After fermentation, cells were removed by centrifugation at 800 RCF (Hermle Z300-K; Germany) for 10 minutes, and the ε-PL was separated and purified from the supernatant using precipitation with sodium tetraphenylborate (NaTPB), following the method adapted from Katano *et al.*[18]

2.3. Fabrication of ECT/ε-PL/PVA

To fabricate biofibers, polyvinyl alcohol (PVA; CAS 9002-89-5, Neutron Chemical, Iran) was dissolved in a 50% ethanol aqueous solution (Merck, USA) at 7.5% w/v. To prevent aggregation, the mixture was heated at 60 °C and stirred continuously for 12 h. Subsequently, ECT (1% w/v) and ε-PL (0.1% w/v) were sequentially incorporated into the PVA solution under constant stirring. The resulting polymer blend was loaded into a 1 mL syringe equipped with a 23-gauge needle for electrospinning. Electrospinning was performed under controlled conditions with the applied voltage of 18 kV, flow rate of 1 mL h^{-1}, and 12 cm distance between the syringe needle and the drum. The obtained ECT/ε-PL/PVA fibers were dried at room temperature for 24 h to remove residual solvent.[19]

2.4. Characterization of ECT/ε-PL/PVA biofibers

2.4.1. Field emission scanning electron microscopy (FE-SEM). The FE-SEM microscopy was utilized to examine the topography and porosity of the electrospun biofibers. The synthesized biofibers were scanned using a QUANTA FEG-450 FE-SEM (FEI, USA), which provided high-resolution images of the fiber morphology.

2.4.2. Attenuated total reflectance-fourier transform infrared spectroscopy (ATR-FTIR). The infrared spectrum of the ECT/ε-PL/PVA biofibers, which enabled a comprehensive understanding of the molecular interactions and structural features within the fiber matrix, was analyzed using ATR-FTIR (JASCO FTIR-6300 spectrometer, Japan) at 4 cm^{-1} resolution across the 350–4000 cm^{-1} range.[20]

2.4.3. Differential scanning calorimetry (DSC). The thermal behavior of ECT/ε-PL/PVA biofibers was analyzed using DSC analysis (Setaram, Model 131 evo, France) under a nitrogen atmosphere. The heating operation was performed in the range of 20–600 °C at a rate of 5 °C min^{-1}.

2.4.4. *In vitro* release of ε-PL. The Itzhaki method was used to investigate the release behavior of ε-PL from the biofiber.[21] For this purpose, a piece of biofiber (1 cm^2) was immersed in 1 mL of PBS (pH 7.2). After the desired time, 100 μl of the prepared solution was added to 2 mL of 1 mM methyl orange and 1.9 mL of PBS. After that, the suspension was placed in a shaking bath at 30 °C for 30 minutes. Then, the samples were centrifuged for 5 minutes at 800 RCF (Hermle Z300-K; Germany), and the absorbance was evaluated using a UV-Vis spectrophotometer at 465 nm (PD-303, Apel, Japan). The cumulative release of ε-PL was estimated by a standard curve. This test was performed in triplicate by three different pieces of biofiber (1 cm^2), and the results are reported as an average.

2.5. Antibacterial activity

The bacterial strains, including *Staphylococcus aureus* ATCC 25923, Methicillin-resistant *S. aureus* ATCC 33591, *Enterococcus faecalis* ATCC 29212, *Streptococcus mutans* ATCC 25175, *Escherichia coli* ATCC 25922, *Klebsiella pneumonia* ATCC 13883, *Serratia marcescens* ATCC 13880, and *Pseudomonas aeruginosa* ATCC 27853, were obtained from the Rah Zist Noavaran Co.

The antibacterial activity of the ECT (100 mg mL^{-1}), ε-PL (10 mg mL^{-1}), PVA (70 mg mL^{-1}), and ECT/ε-PL/PVA microfibers was evaluated using the macrodilution method.[22] The absorbance of the bacterial cultures was measured at 600 nm using UV-Vis spectrophotometer (PD-303, Apel, Japan), and the percentage of the growth inhibition was calculated using formula (1):

$$\text{Growth inhibition (\%)} = (1 - (\text{Abs}_{\text{treated sample}}/\text{Abs}_{\text{control}})) \times 100 \quad (1)$$

2.6. Anti-biofilm activity

To evaluate the inhibitory effect of ECT/ε-PL/PVA biofibers on biofilm formation, a bacterial suspension equivalent to 0.5 McFarland standard was prepared from an overnight culture in PBS. Subsequently, 1 mL of this suspension was inoculated into 149 mL of Tryptic Soy Broth (TSB; Ibresco, Iran) to achieve a final concentration of 1×10^6 CFU mL^{-1}. Then, 0.5 mL of the bacterial suspension was added to each well of the 48-well flat-bottom microplate. A piece of biofiber (1 cm^2) was immersed in each well, and the plate was incubated at 37 °C for 24 hours.

The ability of the biofibers to inhibit biofilm formation was assessed using crystal violet (CV) staining, following the method described by Haney *et al.*, with minor modifications.[23] Briefly, 0.5 mL of 0.01% CV solution (Sigma-Aldrich, USA) was added to each well and incubated at 25 °C for 30 minutes. The CV solution was then removed, and the wells were gently washed three times with 0.5 mL of sterile distilled water to preserve the biofilm. Plates were dried at 60 °C for 30 minutes, after which 0.5 mL of 95% ethanol was added to each well to solubilize the stained biofilm by vigorous pipetting. The OD of the resulting solution was measured at 570 nm using a multi-mode microplate reader (HTX BioTek, USA). The percentage of biofilm inhibition was calculated using the formula (2):

$$\text{Biofilm inhibition (\%)} = (1 - (\text{Abs}_{\text{sample}}/\text{Abs}_{\text{control}})) \times 100 \quad (2)$$

2.7. Radical scavenging activity

The antioxidant potential of ECT/ε-PL/PVA fibers was evaluated by the DPPH (2,2-diphenyl-1-picrylhydrazyl) radical scavenging method.[24] Briefly, a piece of biofiber (1 cm^2) was immersed in 1 mL of 0.2 mM DPPH solution and placed in the dark at 25 °C for 30 minutes. Then, the reduction in DPPH absorbance at 517 nm was measured using a multi-mode microplate reader (HTX BioTek, USA). The percentage of DPPH radical scavenging activity was determined using the following equation.

$$\text{Antioxidant activity (\%)} = (\text{Abs}_{\text{DPPH}} - \text{Abs}_{\text{sample}})/(\text{Abs}_{\text{DPPH}}) \times 100 \quad (3)$$

Ascorbic acid and DPPH solution without biofiber exposure were used as positive and negative controls, respectively.

2.8. Cell cytotoxicity

The cytotoxic effects of ECT/ε-PL/PVA biofibers were investigated on human malignant melanoma cell line (A375), Human Umbilical Vein Endothelial Cells (HUVECs), and mouse fibroblast cells (L929) by MTT assay and flow cytometry analysis. The cells were obtained from the University of Isfahan Cell Line Bank and cultivated in Dulbecco's modified Eagle's minimum media/Nutrient Mixture F-12 (DMEM/F12; BioIdea, Iran), supplemented with 10% fetal bovine serum (BioIdea, Iran) and 1% penicillin–streptomycin solution (Sigma, USA). The cells were seeded into 48-well plates at a density of 10^4 cells cm^{-2} and incubated at 37 °C in 5% CO_2 and 95% humidity for 24 hours before treatment.

The MTT method was conducted according to the Mosmann method to analyze cell viability.[25] Briefly, a piece of biofiber (1 cm^2) was placed into the wells which the cells were seeded and incubated for 24 h. The percentage of cell viability relative to the untreated control was quantified by measuring the absorbance at 570 nm using a multi-mode microplate reader (HTX BioTek, USA) and calculated as follows:

$$\text{Cell viability (\%)} = (\text{Abs}_{\text{treated sample}}/\text{Abs}_{\text{control}}) \times 100 \quad (4)$$

In parallel, flow cytometry was employed to provide a detailed evaluation of cell viability. For this purpose, cells were freshly harvested in DMEM/F12 culture medium and treated with biofibers. The cells were stained with propidium iodide (PI, Merck, Germany) to discriminate viable from non-viable populations. Data acquisition was performed on a Becton Dickinson FACS Calibur flow cytometer, and analysis was conducted using Cell Quest software.

2.9. *In vitro* blood compatibility assay

The hemolysis assay was used to evaluate the blood compatibility of ECT/ε-PL/PVA biofibers.[26] Fresh blood was collected from a healthy volunteer and diluted by adding it to a tube containing 2 mL EDTA and 2.5 mL PBS. The biofibers (1 cm^2) were immersed in 10 mL PBS and incubated in a shaking bath at 37.5 °C. Subsequently, 0.2 mL of the diluted blood solution was added to 0.2 mL of the biofiber suspension and incubated for 1 h. After incubation, the mixture was centrifuged at 100 RCF for 5 min (CF-10; Daihan Scientific, South Korea), and the absorbance of the released hemoglobin in supernatant was measured using a UV-Vis spectrophotometer (PD-303, APEL, Japan) at 540 nm. Deionized water and PBS were used as positive and negative controls, respectively. The hemolysis ratio was calculated from eqn (5):

$$\text{Hemolysis ratio (\%)} = (A_{\text{sample}} - A_{\text{negative control}})/(A_{\text{positive control}} - A_{\text{negative control}}) \times 100 \quad (5)$$

2.10. *In vitro* scratch assay

The scratch assay was conducted to assess the effect of ECT/ε-PL/PVA biofibers on fibroblast cell migration.[27] Initially, 5×10^4 cells were seeded in each well of a 12-well plate containing antibiotic-free DMEM culture medium and allowed to adhere for 24 hours at 37 °C under 5% CO_2 and 95% humidity. Next, a linear scratch was made across the center of each well using a sterile pipette tip. Then, a piece of biofiber (1 cm^2) was placed into each well, and the plate was incubated again for 24 hours. The wells treated with PBS served as a control. After incubation, the wells were gently rinsed three times with PBS, and the cells were fixed in formaldehyde for 1 hour at room temperature. Subsequently, the fixed cells were incubated with a PBS-distilled water mixture for 5 minutes, and the staining process was performed after draining the wells and adding CV solution (diluted 1 : 5 in distilled water) for 20 minutes. Finally, excess stain was removed by thoroughly washing the wells six times with tap water, and migrating cells were visualized and documented under a light microscope at 100× magnification. The extent of wound closure was evaluated by comparing images of treated and control wells with ImageJ analysis software (National Institutes of Health, USA).

2.11. Gene expression analysis during *in vitro* scratch-induced gap closure and migration

The effects of ECT/ε-PL/PVA biofibers on the expression levels of MMP-9, IL-6, TGF-β, and TNF-α as key genes in cell migration and gap closure were investigated *via* quantitative real-time polymerase chain reaction (qRT-PCR).[28,29]

A total of 5×10^4 L-929 cells per well were seeded in a 12-well plate and treated with 1 cm^2 of ECT/ε-PL/PVA biofibers. Then, the cells were incubated at 37 °C with 5% CO_2 and 95% humidity for 24 hours. The total RNA was extracted by MEGARENA RNA extraction kit (Cat no.: FPKT029.0050, KIAGENE FANAVAR, Iran) at 24 hours following the manufacturer's instructions, and cDNA was synthesized from mRNA using cDNA Reverse transcription kit (Cat no.: FPLF012.0050, KIAGENE FANAVAR, Iran). The Quantitative PCR amplification was carried out on Rotor-Gene Q Real-Time PCR Detection System (Biosearch Technologies, USA) using 2 × SYBR Green Real-Time master mixes (Cat no.: FPLF009.1000, KIAGENE FANAVAR, Iran) according to the manufacturer's protocol. The β-actin is used as the internal reference gene to normalize gene expression levels and the sample which treated with PBS was used as control. Data analysis was carried out using the Comparative Threshold Cycle Method and the $2^{-\Delta\Delta Ct}$ formula using REST-2009 software, and statistical significance was evaluated using GraphPad Prism software. Table 1 shows the primers used for qRT-PCR.

Table 1 Primer sequences used for qRT-PCR

Gene	Primer	Primer sequence (5′ → 3′)
β-actin	Forward	GCTCCTAGCACCATGAAGAT
	Reverse	GTGTAAAACGCAGCTCAGTA
MMP-9	Forward	GCCACTACTGTGCCTTTGAGTC
	Reverse	CCCTCAGAGAATCGCCAGTACT
IL-6	Forward	ACTCACCTCTTCAGAACGAATTG
	Reverse	CCATCTTTGGAAGGTTCAGGTTG
TGF-β	Forward	TGAGTATTACAGCAAGGTCCTTG
	Reverse	GGTTCATGTCATGGATGGTGC
TNF-α	Forward	CCTCTCTCTAATCAGCCCTCTG
	Reverse	GAGGACCTGGGAGTAGATGAG

2.12. Ethics approval and consent to participate

The research involving human participants complied with the ethical standards of the Declaration of Helsinki and Good Clinical Practice (GCP) guidelines. Human samples were collected from healthy volunteers after obtaining their informed consent, and the study protocol was approved by the Research Ethics Committee of the University of Isfahan (ethical approval ID: IR-UI-REC.1403.120).

2.13. Statistical analysis

All experiments were performed in triplicate, and all results were presented as the mean value. Under the conventional acceptance of statistical significance, CI was calculated at a confidence level of 95% using GraphPad® Prism software, version 10 (GraphPad Software, USA).

3. Results and discussion

In this study, ECT/ε-PL/PVA was synthesized as a novel bioactive biofiber, and its physicochemical and morphological properties were investigated. Subsequently, antibacterial, antibiofilm, antioxidant, anticancer, and cytotoxic properties of the biofiber were examined. Additionally, the potential of these biofibers as wound dressings was evaluated using hemocompatibility testing, *in vitro* scratch assay, and gene expression analysis during *in vitro* scratch-induced gap closure by qRT-PCR.

3.1. The ECT and ε-PL production

In this study, the production process was optimized to achieve the optimal amount of poly-lysine. The process optimization resulted in the production of 3.5 g L^{-1} of ε-PL in semi-batch culture, which represents a significant improvement in production efficiency compared to non-optimal conditions (0.7 g L^{-1}). The maximum ε-PL production without any optimization has been reported as 1.2 g L^{-1} for *S. albulus* NBRC 4147[30] and 2.3 g L^{-1} for *S. albulus* W-156.[31] Other studies have shown that production can be increased from 0.70 g L^{-1} to 2.89 g L^{-1} in batch culture using wild strains such as *S. albulus* CICC11022 under optimized conditions.[32] However, achieving high-level ε-PL production and progressing toward economically viable industrial applications requires further enhancement of production yield. To date, the highest ε-PL titer reported from an optimized two-stage fermentation with controlled pH is approximately 62.36 g L^{-1} by *Streptomyces* sp. M-Z18,[33] highlighting the significant influence of process engineering on yield improvement.

The reported production of ECT by *H. elongata* under optimized fermentation conditions generally varies between 3 g L^{-1}

and 14–15 g L^{-1}, depending on the strain and cultivation strategy.[34] The ECT titer obtained in the present study was 5 g L^{-1}, confirming the expected fermentation conditions applied for ECT biosynthesis in *H. elongata* IBRC-M 10216. Similarly, Sauer and Galinski achieved 7.4 g L^{-1} ECT using an non-engineered *H. elongata* DSM142 strain through a bacterial milking process, further demonstrating the potential of halo-archaeal systems for efficient ECT production.[35]

3.2. Fabrication and characterization of ECT/ε-PL/PVA

In this study, bioactive ECT/ε-PL fibers were successfully synthesized in a PVA matrix *via* the electrospinning technique. Various studies have used PVA as the main matrix for the synthesis of biofibers and hydrogels. The presence of hydroxyl groups in the PVA structure creates strong hydrogen bonds with other compounds, which facilitates the uniform distribution of additives.[36] Also, the control of permeability and water absorption in PVA biofibers makes this matrix very suitable for medical applications, especially wound dressings that require gas exchange and exudate absorption.[37] Min *et al.*, Fraga *et al.*, and Derakhshankhah *et al.* combined PVA with pullulan, chloramphenicol, and β-cyclodextrin–curcumin, respectively, to fabricate bioactive biofibers with different industrial and biomedical applications.[38–40]

As shown in Fig. 1, the biofibers exhibited a uniform, bead-free structure with a consistent and smooth morphology with a diameter of 0.8 ± 0.157 μm and a pore size of 2.50 ± 1.7 μm. These structural features indicate effective fabrication conducive to potential applications requiring high surface area and porosity. Evaluation of the compound release from the microfiber revealed that each cm^2 contained approximately 3 ± 0.3 mg mL^{-1} of ε-PL and 25 ± 1 mg mL^{-1} of ECT, indicating a homogeneous distribution of these compounds within the biofiber matrix.

The ATR-FTIR spectra that are shown in Fig. 2 indicates molecular interactions between ECT, ε-PL, and PVA, which verifies the formation of a biofiber network. The broad band at 3286.11 cm^{-1} and 3198.36 cm^{-1} is attributed to the stretching vibrations of O–H and N–H groups, which suggest strong intermolecular hydrogen bonding among the polymer matrix and ECT. The peaks at 3018.05 cm^{-1}, 2923.56 cm^{-1}, 2856.1 cm^{-1}, and 2805.92 cm^{-1} correspond to aliphatic C–H stretching vibrations, which are related to the main structures of PVA and ε-PL. A strong absorption at 1733.69 cm^{-1} is assigned to the carbonyl (C═O) group, originating from ECT or acetate groups in PVA. The peaks at 1651.73 cm^{-1} and 1591.95 cm^{-1} are attributed to the amide I (C═O stretching) and amide II (N–H bending and C–N stretching) bands, respectively, confirming the presence of ε-PL and ECT in the biofiber. Further, the peak at 1438.64 cm^{-1} relates to the CH_2 and is typical for aliphatic polymer chains such as PVA, while peaks at 1380.78 cm^{-1} and 1305.57 cm^{-1} are associated with

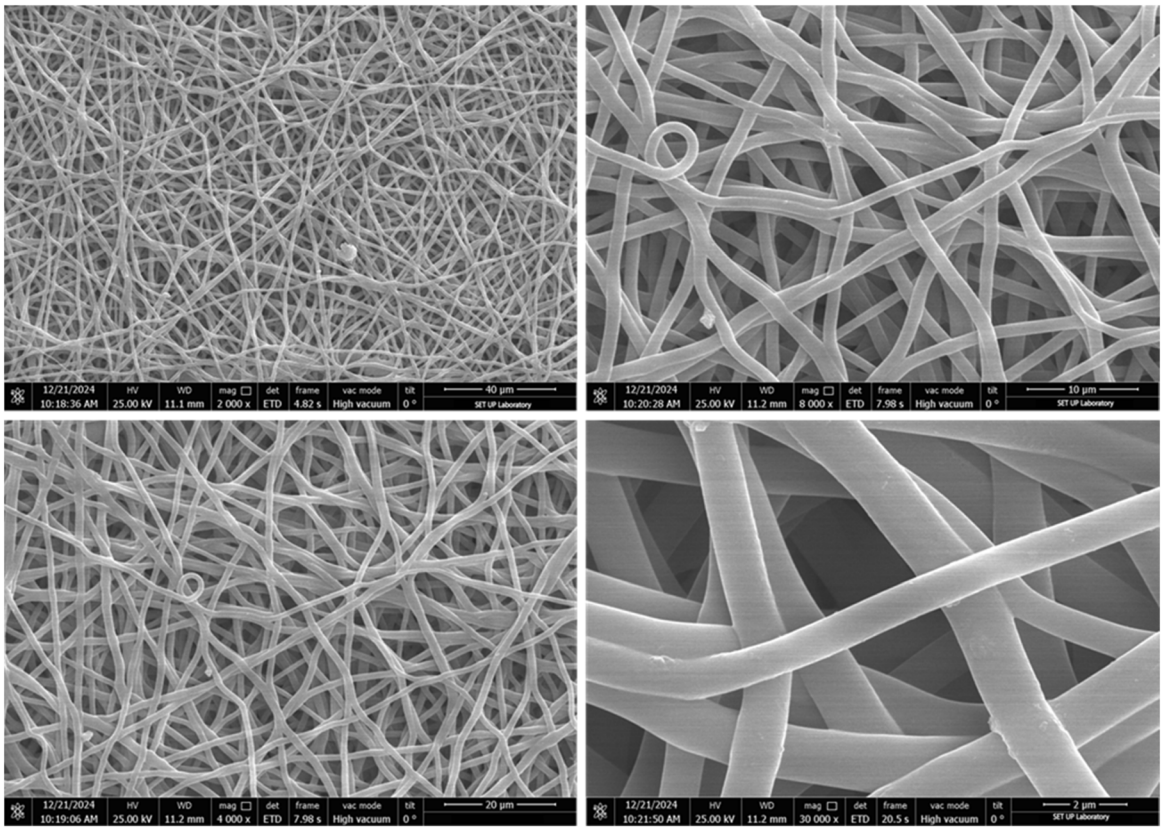

Fig. 1 The FE-SEM image of ECT/ε-PL/PVA biofibers. Biofibers exhibited a bead-free structure with an average diameter of 0.8 ± 0.157 μm and a pore size of 2.50 ± 1.7 μm.

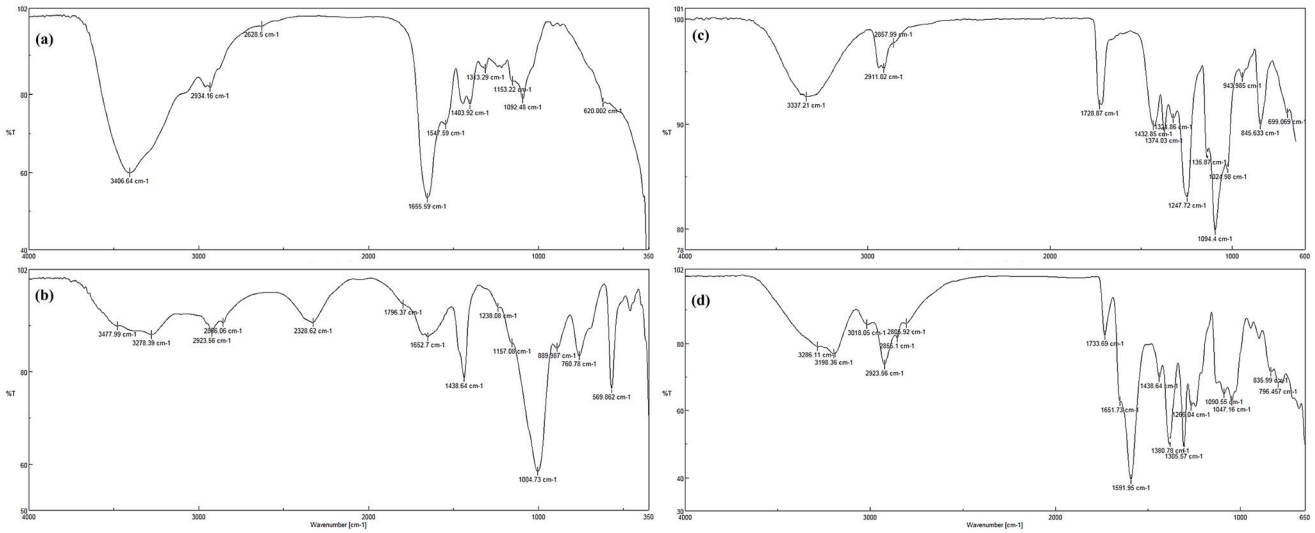

Fig. 2 The ATR-FTIR spectrum of (a) ECT, (b) ε-PL, (c) PVA and (d) ECT/ε-PL/PVA biofiber.

C–H bending, which is related to the polymeric backbone. The peak at 1266.04 cm^{-1} is assigned to C–N stretching, confirming the presence of nitrogen-containing components such as ε-PL and ECT. Additionally, the strong bands at 1090.55 cm^{-1} and 1047.16 cm^{-1} correspond to C–O–C and C–O stretching vibrations, which emphasize on PVA contribution to the composite structure. The peaks at lower wavelengths can be attributed to backbone structures in the composite. Studies demonstrated the presence of hydroxyl, amino, carboxyl, and peptide groups in FTIR analysis of ECT, ε-PL, and PVA serves as evidence for possible intermolecular hydrogen bonding and electrostatic interactions, leading to the regular and stable binding of these three compounds in biofibers.[41–43]

The DSC was used to investigate the thermal properties and compatibility of the ε-PL, ECT, and PVA within the fabricated biofibers. The DSC thermogram of fabricated PVA at same condition exhibits a relatively broad and mild endothermic transition, which can be attributed to the thermal transitions of the polymeric matrix (Fig. 3a). This peak could represent melting of semi-crystalline regions or rearrangement of polymer chains. The limited intensity and enthalpy change (ΔH) of this peak suggest a moderate degree of crystallinity and relatively weak intermolecular interactions within PVA fibers. The absence of multiple or sharp thermal events further indicates a homogeneous polymeric phase without thermally active additives.

The DSC thermogram of ECT/ε-PL/PVA biofiber exhibited three distinct endothermic transitions (Fig. 3b). The first peak at 173.2 °C with an enthalpy change of 8.82 J g^{-1} is related to the glass transition temperature (T_g) or partial recrystallization of the PVA. The prominent peak at 315.35 °C with a substantial enthalpy change of 334.85 J g^{-1}, corresponds to the melting point of the dominant crystalline phase. This peak represents a strong intermolecular interaction between biofiber components and a significant degree of crystallinity and order in its structure.

Finally, the third peak at 439.3 °C with an enthalpy of 13.33 J g^{-1} can be related to the thermal degradation of the biofibers or the breakdown of more thermally stable structural residues. The appearance of this peak emphasizes on enhanced thermal stability of biofibers by the presence of ECT and ε-PL.

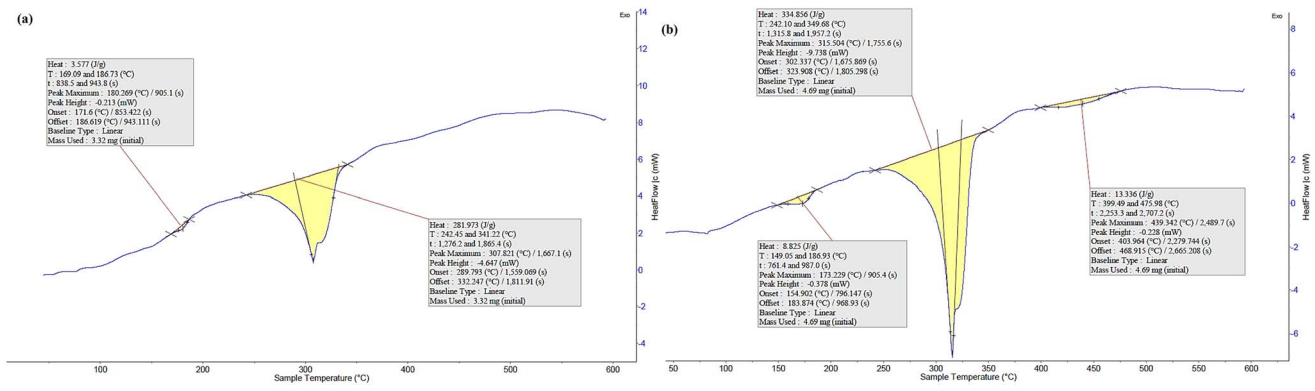

Fig. 3 DSC thermogram of (a) PVA and (b) ECT/ε-PL/PVA fibers. The thermogram of biofiber exhibited three distinct endothermic transitions, which emphasize significant thermal stability, crystallinity, and well-ordered structure of biofiber in comparison with PVA fibers.

The DSC measures the heat flow associated with phase transitions and provides insights into the thermal stability, crystallinity, and molecular interactions of biofiber composites.[44] The increase in T_g and crystallinity percentage in electrospun biofibers observed by DSC indicates the creation of a more stable and orderly structure in the polymer matrix.[45] The electrospinning process, by applying intense tension, causes chain orientation and reduces molecular mobility.[46] It seems that the presence of compounds such as ε-PL or ECT in the synthesized biofibers increases the chain packing density by creating hydrogen bonds and strong intermolecular interactions, ultimately increasing the T_g. These compounds can also act as nucleating agents and facilitate the formation of crystalline regions, leading to increased crystallinity. Such improvements in the thermal and crystalline structure of biofibers provide important functional benefits such as increased mechanical strength, improved thermal stability, reduced swelling, and increased controllability in the release of active molecules, ultimately increasing the efficiency and stability of biofibers in biomedical applications.[47]

The comparative DSC analysis confirms that the incorporation of ε-polylysine and ectoine significantly alters the thermal behavior of the base composite by improving its thermal stability and strengthening intermolecular interactions. These findings indicate that the addition of bioactive agents not only enhances the biological functionality of the microfiber dressing but also improves its physicochemical robustness, making it a promising candidate for biomedical applications such as advanced wound-healing dressings.

3.3. Antibacterial activity

The antibacterial activity of ECT, ε-PL, PVA, and the biofiber composite was evaluated against eight clinically relevant pathogens (Table 2). The inhibition of bacterial growth was measured after 24 hours compared to the control sample. The results showed that ε-PL (10 mg mL^{-1}) had strong antibacterial activity and ECT (100 mg mL^{-1}) had moderate inhibitory effects, while no inhibitory effect was observed from PVA (70 mg mL^{-1}) (p-value<0.05). The synthesized biofibers showed enhanced antibacterial activity compared to the constituent compounds alone and inhibited the growth of almost all bacterial cells, especially methicillin-resistant *S. aureus*, *S. aureus*, *E. faecalis*, *S. mutans*, and *E. coli*. Also, significant inhibition was observed on *P. aeruginosa* (98%), *S. marcescens* (94%), and *K. pneumoniae* (97%).

Analysis of the results revealed that the biofibers possessed a more antibacterial effect against Gram-positive bacteria than Gram-negative bacteria (p-value<0.05). The antimicrobial properties of ε-PL and subsequently the ECT/ε-PL/PVA composite are attributed to the cationic nature of this polypeptide.[48] This compound affects the cell membrane components, increasing the permeability and reducing polarity, which leads to the release of cellular components such as proteins and ions. These interactions lead to cell wall destruction and ultimately cell death.[14,49]

Also, the results indicate that the integration of ECT and ε-PL into the biofiber matrix enhances the antibacterial performance and makes it a promising candidate in various industries, especially wound dressing and packaging materials. Various studies have shown that ECT, as a compatible solute, stabilizes biological molecules through its strong water-binding capacity and the formation of a hydration shell.[42,50] This stabilizing effect appears to improve the durability and functional longevity of ε-PL, which disrupts bacterial cell membranes through electrostatic interactions.

3.4. Anti-biofilm activity

The anti-biofilm activities of ECT, ε-PL, PVA, and the ECT/ε-PL/PVA biofibers were evaluated using crystal violet staining. The ε-PL exerts its antibacterial and antibiofilm effects through strong electrostatic interactions with negatively charged bacterial cell membranes, ultimately leading to membrane disruption and loss of cellular integrity.[51] In addition to its direct microbicidal action, ε-PL interferes with early biofilm formation by inhibiting bacterial adhesion, suppressing exopolysaccharide biosynthesis, and downregulating genes involved in motility, flagella assembly, and extracellular matrix production, thereby destabilizing both developing and established biofilms.[52,53] In contrast, ECT functions as a compatible solute and chemical chaperone that stabilizes proteins and lipid bilayers while enhancing surface hydration.[54] Although ectoine does not possess strong antimicrobial activity, it can reduce bacterial

Table 2 Bacterial growth inhibition (%) by ECT, ε-PL, PVA, and ECT/ε-PL/PVA biofibers

	Bacterial growth inhibition (%)			
Bacteria	ECT (100 mg mL^{-1})	ε-PL (10 mg mL^{-1})	PVA (70 mg mL^{-1})	ECT/ε-PL/PVA (25/3/20 mg mL^{-1})
Methicillin-resistant *S. aureus* (MRSA)	50.10	98.15	2.00	>99.00
S. aureus	54.70	98.40	2.00	>99.00
E. faecalis	47.50	97.00	3.00	>99.00
S. mutans	48.55	98.20	1.00	>99.00
P. aeruginosa	40.46	93.80	2.00	98.00
E. coli	42.33	100.00	2.00	>99.00
S. marcescens	38.40	90.30	3.00	94.00
K. pneumoniae	41.94	94.90	2.00	97.00
p-Value	0.001			

attachment and improve the physicochemical environment of biomaterials, facilitating controlled release and deeper penetration of co-delivered antimicrobial agents.[55] The co-incorporation of ε-PL and ectoine generates a multifunctional biofiber platform that exhibits markedly enhanced antibiofilm activity and broad-spectrum antibacterial performance compared with fibers containing only a single antimicrobial component.[56]

The results in Table 3 indicate that biofibers significantly inhibited the biofilm of Gram-negative bacteria more than Gram-positive bacteria (p-value<0.05). It could be due to the difference in the composition of the biofilm matrix and the bacterial cell wall. The innovative co-incorporation of ε-PL and ECT improves physicochemical characteristics of biofibers, which enable better penetration and even distribution of antimicrobials. The ECT/ε-PL/PVA biofibers inhibited Methicillin Resistant *S. aureus* (MRSA), *S. aureus*, *E. faecalis*, *S. mutans*, *P. aeruginosa*, *E. coli* biofilms by 81, 83, 83, 84, 89, 91, 94, and 91%, respectively.

3.5. Radical scavenging activity

Reactive oxygen species (ROS) are essential for normal wound healing, but when they accumulate in excess, they can cause serious damage. For this reason, the presence of antioxidant compounds is important during the wound healing process.[57] By controlling the presence of ROS and modulating cellular activity, antioxidants allow for a smoother transition from the inflammatory, proliferative, and regenerative phases of wound healing.[58] Antioxidant dressings or treatments can also reduce inflammation and biofilm formation, which supports faster and more effective wound healing.[59] In this study, the antioxidant activity of synthesized biofibers was assessed using the DPPH radical scavenging assay (Fig. 4). The results demonstrated that the ECT/ε-PL/PVA biofibers exhibited significantly higher antioxidant capacity compared to ECT, ε-PL, PVA, and even ascorbic acid (1 mg mL^{-1}) as a positive control (p-value<0.05). The radical scavenging activity of ECT, ε-PL, PVA, and synthesized biofibers was 27, 78, 15, and 89%, respectively.

As a positively charged biopolymer, ε-PL can electrostatically interact with negatively charged molecules such as free radicals and exhibit antioxidant and anticancer properties.[48] As demonstrated in this study, the ε-PL and ECT incorporated within the ECT/ε-PL/PVA biofibers exhibited strong antioxidant properties, highlighting an additional beneficial feature of these biofibers for use as effective wound dressings.

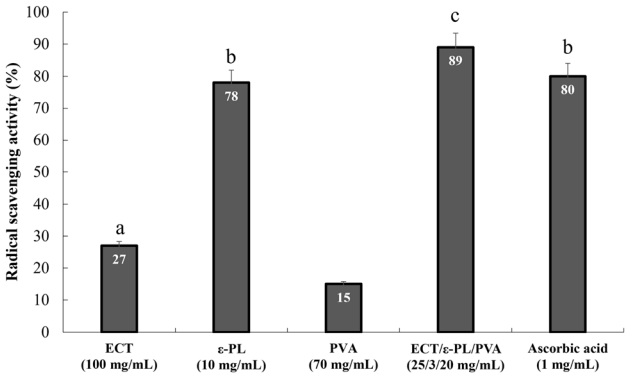

Fig. 4 DPPH radical scavenging activity of ECT, ε-PL, PVA, and ECT/ε-PL/PVA biofibers. Ascorbic acid (1 mg mL^{-1}) was used as the positive control. Alphabetical differences (a–c) indicate statistically significant differences between variables at the 95% statistical level.

3.6. Cytotoxicity evaluation

The results demonstrated a marked cytotoxic effect of the ECT/ε-PL/PVA biofibers on A375 cells, with more than a 90% reduction in cell viability after 24 and 48 h of exposure. Statistical analysis confirmed that the viability of A375 cells treated with the composite biofibers or ε-PL alone was significantly lower than those treated with ECT or PVA (p-value<0.05) (Fig. 5). In contrast, all tested materials, including ECT, ε-PL, PVA, and the ECT/ε-PL/PVA biofibers, maintained high viability (>90%) in normal L929 fibroblasts and HUVEC endothelial cells, showing no significant differences among the groups (p-value>0.05). Quantitatively, after 24 h of treatment, ECT (100 mg mL^{-1}), ε-PL (10 mg mL^{-1}), and PVA (70 mg mL^{-1}) decreased A375 cell viability by approximately 30%, 75%, and 5%, respectively, whereas the ECT/ε-PL/PVA biofibers reduced viability by more than 90%.

Several studies have shown that the ε-PL exhibits anticancer activity by inducing apoptosis and inhibiting cell proliferation

Table 3 Biofilm inhibition (%) by ECT, ε-PL, PVA, and biofibers

	Biofilm inhibition (%)			
Bacteria	ECT (100 mg mL^{-1})	ε-PL (10 mg mL^{-1})	PVA (70 mg mL^{-1})	ECT/ε-PL/PVA (25/3/20 mg mL^{-1})
Methicillin-resistant *S. aureus* (MRSA)	34	78	—	81
S. aureus	38	79	—	83
E. faecalis	33	76	—	83
S. mutans	32	77	—	84
P. aeruginosa	28	83	—	89
E. coli	31	85	—	91
S. marcescens	26	84	—	94
K. pneumoniae	27	79	—	91
p-Value	0.001			

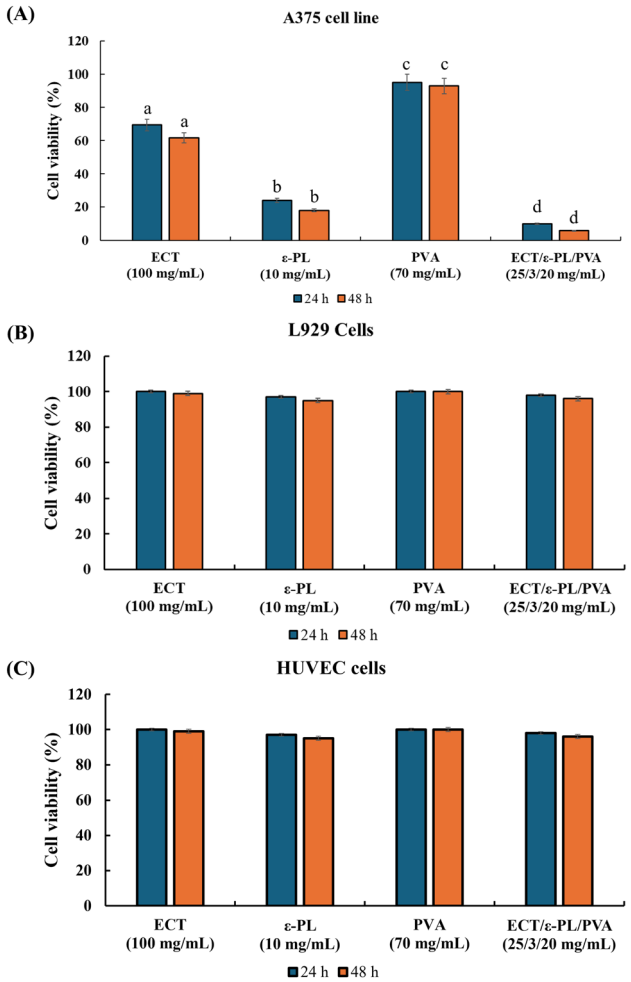

Fig. 5 Evaluation of the ECT, ε-PL, PVA, and ECT/ε-PL/PVA biofibers cell cytotoxicity against (A) human malignant melanoma A375 cell line, (B) L929 fibroblast cells, and (C) Human Umbilical Vein Endothelial Cells (HUVECs) by MTT test. Alphabetical differences (a, b and …) indicate statistically significant differences between variables at the 95% statistical level.

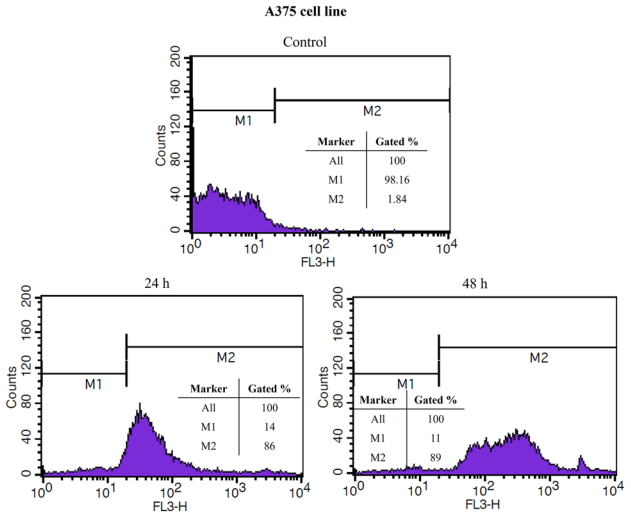

Fig. 6 Flow cytometry histograms of A375 cells after 24 h treatment with ECT/ε-PL/PVA biofibers. The M1 and M2 zones show living and dead cells gated respectively.

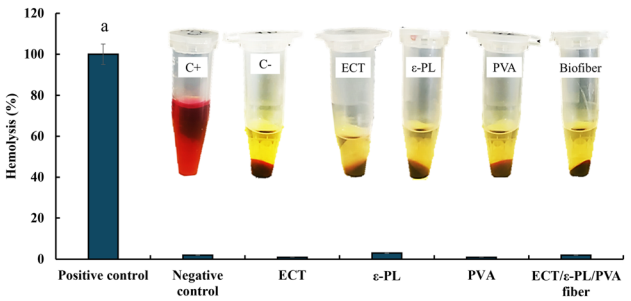

Fig. 7 Hemolytic activity of ECT, ε-PL. PVA and ECT/ε-PL/PVA biofibers on human red blood cells. Alphabetical differences (a, b and …) indicate statistically significant differences between variables at the 95% statistical level.

and angiogenesis in various cancer cell lines and tumor models.[15,60,61] Additionally, ECT has been reported to either promote apoptosis in cancer cells or protect non-cancerous cells from stress.[62,63] This dual behavior suggests that ECT may selectively induce cancer cell death while preserving normal cell viability.[64] The MTT and flow cytometry results of the present study also showed that the combined incorporation of ε-PL and ECT in the biofiber composition not only protects healthy cells but also effectively induces cell death in cancer cells. Flow cytometric analysis also showed that ECT/ε-PL/PVA biofibers reduced A375 cell viability by 86% and 89% after 24 and 48 h, respectively (Fig. 6). These results were as expected and consistent with the MTT results, confirmed the anticancer effects of the synthesized biofibers.

3.7. *In vitro* blood compatibility assay

The hemocompatibility of the biofibers was investigated using anticoagulated human blood (Fig. 7). The results demonstrated that the biofibers induced less than 2% hemolysis of red blood cells, which is well within the non-hemolytic threshold defined by the ISO 10993-4 standard. In addition, the individual components (ECT, ε-PL, and PVA) also induced less than 2% hemolysis, with no statistically significant difference compared to the synthesized biofibers (p-value>0.05). These findings indicate the excellent biofibers hemocompatibility which supports their safe application in biomedical industries.

3.8. *In vitro* scratch assay

Wound healing is a complex, multi-stage process involving cell migration, proliferation, matrix remodeling, inflammation, and angiogenesis.[65] Re-epithelialization refers to the phase in which epithelial cells migrate from the wound edges across the wound bed to cover it, mainly during the proliferative phase of healing. Additionally, fibroblast cells migrate to the wound site after injury to produce extracellular matrix components and support tissue regeneration.[66] Therefore, cell migration is essential for overall wound closure, restoring the epidermal barrier, and

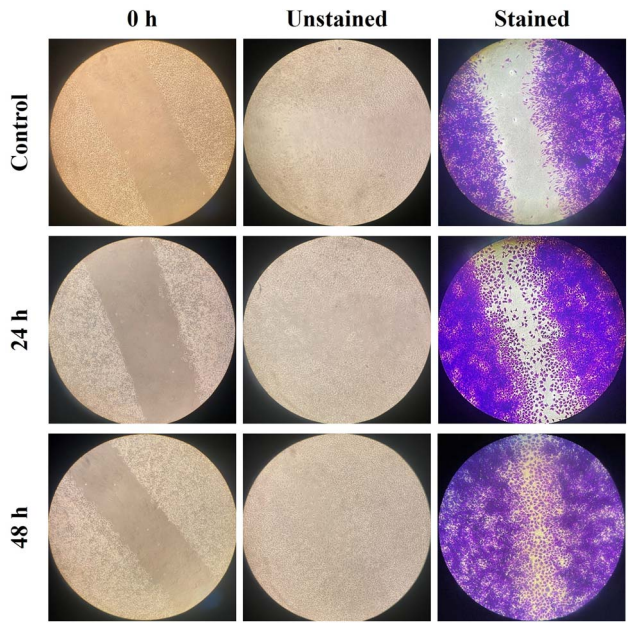

Fig. 8 Cell migration and gap closure ability in L929 cells treated with ECT/ε-PL/PVA biofibers. Results indicate that more than 95% of the space is closed with high cell density after 48 hours of treatment.

forming new tissue. The L929 fibroblast cells migration which treated with ECT/ε-PL/PVA microfibers was evaluated using an *in vitro* scratch assay, and the results were analyzed using ImageJ software (Fig. 8).

The results showed that treatment of fibroblast cells with synthesized biofibers promoted the early phase of wound healing and more than 75% gap closure within 24 hours. The gap closure was increased significantly after 48 hours, reaching more than 98% while the gap closure in samples treated with PBS as a control was less than 10%.

Qaria *et al.* reported that ECT partially inhibits the migration of human HaCaT keratinocyte cells while suppressing cancer cell proliferation through the modulation of genes involved in epigenetic regulation.[62] Lin *et al.* demonstrated that ε-PL, used as a surface adhesive agent without harming cell viability, enhances the migration of mouse embryonic fibroblast cells (NIH 3T3), thereby promoting wound healing.[67] Based on these studies and the present research, it can be concluded that ε-PL and ECT support wound healing at different levels. ε-PL helps wound repair by providing a supportive surface that encourages cell migration and attachment, while ECT influences the process at the molecular level through regulation of signaling pathways.

In recent years, bioactive compounds have been used with different matrices to produce hydrogels or multifunctional biofibers to advance wound healing, especially for diabetic or burn wounds. In this study, ECT/ε-PL/PVA biofibers were synthesized *via* electrospinning for the first time to evaluate the synergistic effects of these compounds on wound healing. In this biofiber, ECT promotes cellular protection and healing, ε-PL delivers antimicrobial activity, and PVA, as a biocompatible and electrospinnable polymer matrix, ensures mechanical stability and facilitates the uniform dispersion of both bioactive molecules within the microfiber structure.

Wang *et al.* showed that adding ECT to wound dressings can effectively remove the surface hydration layer and absorb wound exudate.[55] This approach may appear somewhat contentious, as increased moisture within the wound environment can create conducive conditions for microbial colonization and subsequent infection. However, the integration of antimicrobial or antibiofilm agents, such as antimicrobial peptides, significantly enhances the efficacy of the dressing. By maintaining an optimal moisture, this method facilitates improved wound healing and effectively promotes the migration of epithelial cells to the wound site.

Zarrintaj *et al.*, who studied ε-PL-based biomaterials, concluded that ε-PL can play a protective role in increasing the lifespan of skin tissue by minimizing the appearance of damaged skin.[68] It has also been proven in previous studies that ε-PL, as an antimicrobial peptide, can be effective against a wide range of microorganisms.[14] It seems that aligning these studies with the results of Zarrintaj *et al.* can introduce ε-PL not only as an antimicrobial and antioxidant compound but also as a regenerative agent. In this study, we demonstrated that the simultaneous use of ε-PL and ECT can have a profound effect on wound healing at the laboratory level.

3.9. Gene expression analysis during *in vitro* scratch-induced gap closure and migration

At the molecular level, various signaling molecules such as growth factors (*e.g.*, TGF-β, HGF), cytokines (*e.g.*, IL-6, TNF-α), and matrix metalloproteinases (MMPs) regulate cell proliferation, migration, inflammation, and ECM remodeling. Effective healing requires a delicate balance of inflammation and its timely resolution, efficient re-epithelialization, and balanced ECM turnover, all coordinated by inflammatory cells, keratinocytes, fibroblasts, and endothelial cells.[66] Understanding cellular interactions and molecular pathways is crucial for developing wound healing strategies and reducing pathological outcomes. Therefore, in this study, the expression levels of MMP-9, TGF-β, IL-6, and TNF-α were analyzed using qRT-PCR to explain their roles in the healing process. The results revealed that the expression of MMP-9 and TGF-β in L929 cells which treated with the ECT/ε-PL/PVA biofibers for 24 hours were significantly increased compared to the control while the expression of IL-6 and TNF-α were decreased (Fig. 9) (p-value<0.05).

The MMP-9 showed a statistically significant increase in expression, more than a 5-fold change relative to the control (p-value<0.05). The expression of TGF-β also increased by more than 3-fold, which was significantly higher than control (p-value<0.05). Although the expression levels of the IL-6 and TNF-α genes exhibited less than a one-fold change relative to the control group, a statistically significant downregulation of TNF-α gene expression was observed compared with the control (p-value<0.05). In contrast, no significant difference was detected in IL-6 gene expression between the treated and control (p-value>0.05).

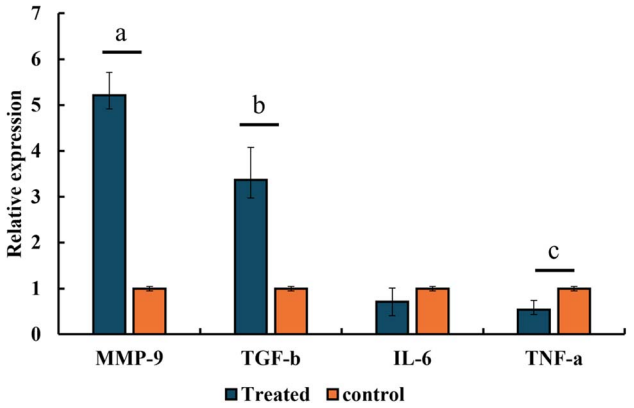

Fig. 9 The expression level of gap closure and migration involved genes in L929 cells which treated by ECT/ε-PL/PVA fibers for 24 hours. The β-actin is used as the internal reference gene to normalize gene expression levels and the L929 cells treated with PBS was used as control. Alphabetical differences (a, b, …) indicate statistically significant differences between treated sample and control at the 95% statistical level.

In agreement with these findings and the results of the scratch assay, the modest increase in IL-6 and TNF-α expression appears to be attributed to the presence of ECT in the biofiber, which reduces inflammation, modulates inflammatory cytokine expression, and ultimately promotes tissue repair while accelerating wound healing.

Furthermore, the results showed that the expression of MMP-9 and TGF-β, which play important roles in degrading ECM components and facilitating cell migration, increased significantly during the cell proliferation phase, possibly due to the presence of ε-PL in the ECT/ε-PL/PVA biofiber. Meanwhile, the expression of inflammatory molecules IL-6 and TNF-α decreased significantly after 24 hours, likely due to the anti-inflammatory effects of ECT compared to MMP-9 and TGF-β. Li *et al.* reported that ECT can significantly suppress the expression of TNF-α, IL-1β, IL-6, and IL-8 in damaged primary human corneal epithelial cells (HCECs), highlighting the potential of ECT in protecting and restoring epithelial cells.[69]

4. Conclusions

In this study, electrospun biofibers composed of ECT, ε-PL, and PVA with a uniform structure and diameter of 0.8 ± 0.157 μm were successfully fabricated. The main innovation of this work lies in the novel combination of the complementary properties of ECT and ε-PL, which results in the first-ever production of ECT/ε-PL/PVA microfibers. These biofibers demonstrated excellent antibacterial, antibiofilm, antioxidant, anticancer, and biocompatible characteristics. Furthermore, they effectively promoted fibroblast migration and modulated the expression of critical wound healing-related genes in experimental assessments. The synergistic interaction of ECT and ε-PL significantly enhances the healing process while reducing inflammation. Overall, the findings highlight the promising potential of these microfibers as bioactive, hemo-compatible, and multifunctional wound dressings for advanced medical applications. Although the wound dressing developed in this study demonstrated excellent performance, further evaluations are still required to fully establish its safety and efficacy for clinical use. Among these, comprehensive *in vivo* investigations are particularly crucial, and future research should prioritize such studies to advance the translational potential of this promising biomaterial.

Author contributions

H. Hagh Ranjbar: validation, methodology, formal analysis, investigation, data curation, writing – original draft. A. Hosseini Abari: supervision, methodology, formal analysis, investigation, writing – review & editing.

Conflicts of interest

There are no conflicts to declare.

Data availability

The datasets generated and/or analyzed during the current study are available within the article, and the raw data are available from the corresponding author upon reasonable request.

Supplementary information (SI) is available. See DOI: https://doi.org/10.1039/d5ra09550f.

Acknowledgements

We thank the University of Isfahan for the financial support given to the PhD student for a training period in the Department of Cell and Molecular Biology and Microbiology, University of Isfahan.

References

1 T. Manu, A. R. Nazmi, B. Shahri, N. Emerson and T. Huber, *Mater. Today Commun.*, 2022, **31**, 103308.
2 M. Akter, M. H. Uddin and I. S. Tania, *J. Reinf. Plast. Compos.*, 2022, **41**, 705–742.
3 M. Ramesh, L. Rajeshkumar, D. Balaji and V. Bhuvaneswari, *Curr. Anal. Chem.*, 2023, **19**, 38–69.
4 D. Ji, Y. Lin, X. Guo, B. Ramasubramanian, R. Wang, N. Radacsi, R. Jose, X. Qin and S. Ramakrishna, *Nat. Rev. Methods Primers*, 2024, **4**, 1.
5 A. Nadaf, A. Gupta, N. Hasan, S. Ahmad, P. Kesharwani and F. J. Ahmad, *RSC Adv.*, 2022, **12**, 23808–23828.
6 R. Mazzoli, K. Riedel and E. Pessione, *Bioactive compounds from microbes*, Frontiers Media SA, 2017, p. 392.
7 P. Monciardini, M. Iorio, S. Maffioli, M. Sosio and S. Donadio, *Microb. Biotechnol.*, 2014, **7**, 209–220.
8 M. Liu, H. Liu, M. Shi, M. Jiang, L. Li and Y. Zheng, *Microb. Cell Factories*, 2021, **20**, 76.
9 Z. Ma, C. Wu, L. Zhu, R. Chang, W. Ma, Y. Deng and X. Chen, *3 Biotech*, 2022, **12**, 331.

10 M. Di Gioacchino, F. Bruni, A. Sodo, S. Imberti and M. A. Ricci, *Mol. Phys.*, 2019, **117**, 3311–3319.
11 Y. Chen, W. Miao, X. Li, Y. Xu, H. Gao and B. Zheng, *Trends Food Sci. Technol.*, 2023, **139**, 104131.
12 L. Wang, C. Zhang, J. Zhang, Z. Rao, X. Xu, Z. Mao and X. Chen, *Front. Bioeng. Biotechnol.*, 2021, **9**, 748976.
13 N. A. Patil and B. Kandasubramanian, *Eur. Polym. J.*, 2021, **146**, 110248.
14 H. Hagh Ranjbar, A. Hosseini-Abari, S. M. Ghasemi and Z. Hafezi Birgani, *Microbiology*, 2023, **169**, 001363.
15 H. H. Ranjbar, A. H. Abari, S. M. Ghasemi and N. Ghorbani, *Biotechnol. Bioprocess Eng.*, 2022, **27**, 586–595.
16 S. Li, Y. Mao, L. Zhang, M. Wang, J. Meng, X. Liu, Y. Bai and Y. Guo, *Biotechnol. Biofuels Bioprod.*, 2022, **15**, 65.
17 Y.-H. Wei, F.-W. Yuan, W.-C. Chen and S.-Y. Chen, *J. Biosci. Bioeng.*, 2011, **111**, 336–342.
18 H. Katano, T. Yoneoka, N. Kito, C. Maruyama and Y. Hamano, *Anal. Sci.*, 2012, **28**, 1153–1157.
19 Z. Renkler, I. Cruz Maya and V. Guarino, *Fibers*, 2023, **11**, 85.
20 L. Sriphong, T. Rojanarata, C. Gasser and B. Lendl, *TJPS*, 2018, 42.
21 R. F. Itzhaki, *Anal. Biochem.*, 1972, **50**, 569–574.
22 M. Balouiri, M. Sadiki and S. K. Ibnsouda, *J. Pharm. Anal.*, 2016, **6**, 71–79.
23 E. F. Haney, M. J. Trimble and R. E. Hancock, *Nat. Protoc.*, 2021, **16**, 2615–2632.
24 İ. Gulcin and S. H. Alwasel, *Processes*, 2023, **11**, 2248.
25 T. Mosmann, *J. Immunol. Methods*, 1983, **65**, 55–63.
26 A. Bhatt, R. P. Nair, R. Raju and R. Geeverghese, in *Biomedical Product and Materials Evaluation*, Elsevier, 2022, pp. 435–459.
27 S. Balko, E. Kerr, E. Buchel, S. Logsetty and A. Raouf, *Methods Protoc.*, 2023, **6**, 87.
28 C. Qing, *Chin. J. Traumatol.*, 2017, **20**, 189–193.
29 B. Behm, P. Babilas, M. Landthaler and S. Schreml, *J. Eur. Acad. Dermatol. Venereol.*, 2012, **26**, 812–820.
30 S. C. Shukla and A. Mishra, *APCBEE Proc.*, 2012, **2**, 120–124.
31 L. Wang, X. Chen, G. Wu, X. Zeng, X. Ren, S. Li, L. Tang and Z. Mao, *Appl. Biochem. Biotechnol.*, 2016, **180**, 1601–1617.
32 Y. Yu, L. Xia and J. Wen, *Biochem. Eng. J.*, 2025, 109758.
33 X.-D. Ren, Y.-J. Xu, X. Zeng, X.-S. Chen, L. Tang and Z.-G. Mao, *RSC Adv.*, 2015, **5**, 82138–82143.
34 P. Fatollahi, M. Ghasemi, F. Yazdian and A. Sadeghi, *Biotechnol. Prog.*, 2021, **37**, e3073.
35 T. Sauer and E. A. Galinski, *Biotechnol. Bioeng.*, 1998, **57**, 306–313.
36 G. C. Türkoğlu, N. Khomarloo, E. Mohsenzadeh, D. N. Gospodinova, M. Neznakomova and F. Salaün, *Int. J. Mol. Sci.*, 2024, **25**, 1668.
37 E. Uslu, M. Gavgali, M. O. Erdal, Ş. Yazman and L. Gemi, *Mater. Today Commun.*, 2021, **26**, 101939.
38 T. Min, X. Sun, L. Zhou, H. Du, Z. Zhu and Y. Wen, *Carbohydr. Polym.*, 2021, **270**, 118391.
39 H. Derakhshankhah, R. E. Malekshah, Z. Izadi, M. Samari, M. Rezaee and H. Samadian, *J. Mol. Liq.*, 2023, **386**, 122500.
40 G. N. Fraga, D. C. Dragunski, B. H. Vilsinski, C. K. da Silva Azevedo, H. J. Wiggers, M. G. I. Faria, J. Caetano, M. R. da Costa, V. S. Zanuto and A. R. S. Rossin, *Colloids Surf., A*, 2023, **674**, 131760.
41 F. Hakimi, H. Balegh, F. Kazeminava, S. Moradi, M. Eskandari and Z. Ahmadian, *Heliyon*, 2024, **10**(15), e35264.
42 A. Tyara Simbara, F. Faridatul Habibah and R. Hertadi, *ACS Omega*, 2025, **10**, 12200–12213.
43 C. Berthomieu and R. Hienerwadel, *Photosynth. Res.*, 2009, **101**, 157–170.
44 J. M. Lynch, R. N. Corniuk, K. C. Brignac, M. R. Jung, K. Sellona, J. Marchiani and W. Weatherford, *Environ. Pollut.*, 2024, **346**, 123607.
45 D. Mileva, D. Tranchida and M. Gahleitner, *Polym. Cryst.*, 2018, **1**, e10009.
46 M. S. Islam, B. C. Ang, A. Andriyana and A. M. Afifi, *SN Appl. Sci.*, 2019, **1**, 1248.
47 E. J. Torres-Martínez, J. M. Cornejo Bravo, A. Serrano Medina, G. L. Pérez González and L. J. Villarreal Gómez, *Curr. Drug Delivery*, 2018, **15**, 1360–1374.
48 E. Lebaudy, C. Guilbaud-Chéreau, B. Frisch, N. E. Vrana and P. Lavalle, *Adv. NanoBiomed Res.*, 2023, **3**, 2300080.
49 M. Hyldgaard, T. Mygind, B. S. Vad, M. Stenvang, D. E. Otzen and R. L. Meyer, *Appl. Environ. Microbiol.*, 2014, **80**, 7758–7770.
50 M. Borjian Boroujeni, M. R. Aghamaali, H. Naieri and K. Beheshti-Maal, *Microbiol. Biotechnol. Lett.*, 2023, **6**, 17–36.
51 D.-U. Lee, Y. J. Park, H. H. Yu, S.-C. Jung, J.-H. Park, D.-H. Lee, N.-K. Lee and H.-D. Paik, *Foods*, 2021, **10**, 2211.
52 J. Kang, X. Zhang, Y. Huang, Y. Zhu, L. Liu, B. Sun, M. Qu and X. Zhu, *Food Biosci.*, 2025, **66**, 106314.
53 S. Wu, Q. Jiang, D. Lu, X. Zhai, J. Duan and B. Hou, *npj Mater. Degrad.*, 2024, **8**, 122.
54 L. Czech, L. Hermann, N. Stöveken, A. A. Richter, A. Höppner, S. H. Smits, J. Heider and E. Bremer, *Genes*, 2018, **9**, 177.
55 X. Wang, R. Mu, Y. Zhou, J. Li, Q. Ma, J. Wang, Y. Ma, W. Sheng, X. Hu and F. Zhou, *Adv. Funct. Mater.*, 2025, 2423356.
56 G. Amariei, V. Kokol, V. Vivod, K. Boltes, P. Letón and R. Rosal, *Int. J. Pharm.*, 2018, **553**, 141–148.
57 K. Ukaegbu, E. Allen and K. K. Svoboda, *Int. Wound J.*, 2025, **22**, e70330.
58 T. Zivari-Ghader, M.-R. Rashidi and M. Mehrali, *Int. J. Biol. Macromol.*, 2024, **279**, 134578.
59 I. M. Comino-Sanz, M. D. López-Franco, B. Castro and P. L. Pancorbo-Hidalgo, *J. Clin. Med.*, 2021, **10**, 3558.
60 Y.-F. Chen, A.-L. Shiau, S.-J. Chang, N.-S. Fan, C.-T. Wang, C.-L. Wu and J.-S. Jan, *Acta Biomater.*, 2017, **55**, 283–295.
61 S. Debnath, S. Karan, M. Debnath, J. Dash and T. K. Chatterjee, *Asian Pac. J. Cancer Prev.*, 2017, **18**, 2255.
62 M. A. Qaria, C. Xu, R. Hu, R. A. Alsubki, M. Y. Ali, S. Sivasamy, K. A. Attia and D. Zhu, *Mar. Drugs*, 2023, **21**, 621.
63 S. Xu, P. Zhang, L. Qiao, G. Shen, Y. Li and D. Zhu, *Biomed. Res. Ther.*, 2025, **12**, 7621–7632.
64 M. Sheikhpour, A. Sadeghi, F. Yazdian, A. Movafagh and A. Mansoori, *Stress*, 2019, **16**, 20–23.

65 O. A. Peña and P. Martin, *Nat. Rev. Mol. Cell Biol.*, 2024, **25**, 599–616.
66 A. A. Mamun, C. Shao, P. Geng, S. Wang and J. Xiao, *Front. Immunol.*, 2024, **15**, 1395479.
67 J.-Y. Lin, K.-Y. Lo and Y.-S. Sun, *Materials*, 2019, **12**, 2775.
68 P. Zarrintaj, S. Ghorbani, M. Barani, N. P. Singh Chauhan, M. Khodadadi Yazdi, M. R. Saeb, J. D. Ramsey, M. R. Hamblin, M. Mozafari and E. Mostafavi, *Bioeng. Transl. Med.*, 2022, **7**, e10261.
69 J.-M. Li, N. Lin, Y. Zhang, X. Chen, Z. Liu, R. Lu, F. Bian, H. Liu, S. C. Pflugfelder and D.-Q. Li, *Ocul. Surf.*, 2024, **32**, 182–191.